Damir ŽARKO, Stjepan FRLJIĆ, Stjepan STIPETIĆ

University of Zagreb Faculty of Electrical Engineering and Computing

doi:10.15199/48.2016.12.46

Design of Premium Efficiency (IE3) Induction Motors Using Evolutionary Optimization and Scaling Laws

Abstract. *The paper presents a method for optimal design of premium efficiency (IE3) squirrel-cage induction motor by utilizing radial scaling, axial scaling and rewinding of an existing 4 kW 4-pole high efficiency (IE2) motor. The scaling factors are defined for all parameters of the equivalent circuit and consider the influence of saturation on main and leakage inductances in all operating points. The optimal scaling factors are determined using Differential evolution optimization algorithm with minimum volume of iron stack defined as a cost function.*

Streszczenie. *W artykule zaprezentowano metodę optymalnego projektowania silnika indukcyjnego klatkowego w standardzie IE3 poprzez wykorzystanie skalowania promieniowego, osiowego oraz przezwojenia istniejącego silnika czterobiegunowego o mocy 4 kW w standardzie IE2. Współczynniki skalowania zdefiniowane zostały dla wszystkich parametrów obwodu zastępczego. Został rozważony wpływ nasycenia na indukcyjności: główną I rozproszenia we wszystkich punktach działania. Optymalne współczynniki skalowania są określone za pomocą algorytmu optymalizacyjnego ewolucji różniczkowej z minimalną objętością ferromagnetyka zdefiniowaną jako funkcja kosztu.(**Projektowanie silników indukcyjnych w standardzie IE3 za pomocą optymalizacji ewolucyjnej I praw skalowania)*

Keywords: induction motor, scaling laws, optimization
Słowa kluczowe: silnik indukcyjny, prawa skalowania, optymalizacja

Introduction

Industrial induction motors are the major consumers of electric energy in developed countries and account for about 40% of overall power consumption globally [1]. The new premium efficiency standard (IE3) for induction motors rated 7.5 to 375 kW has been in effect in the European Union since January 1, 2015 and is defined by the IEC 60034-30 standard [2].

The classical and least expensive approach which manufacturers use to redesign their existing motors to comply with IE3 standard is to extend the length of the lamination stack and rewind the stator in order to minimize the sum of copper and iron losses [3]. This process suffers from several constraints. The maximum stack length is limited by the length of the existing die cast aluminium or iron frames that manufacturers normally use. In some cases axial extension is not sufficient so motor size must be increased radially as well to reach the IE3 efficiency level. Bone [4] compared induction machine scaling based on the preservation of the slot current density with scaling based on the preservation of the linear current density along stator bore. Stipetic *et. al.* [5] explored the radial and axial scaling of brushless PM motors and derived exact analytical relations that are used to derive the performance parameters of the scaled machine using parameters of the original machine combined with geometrical factors of axial scaling, radial scaling, and rewinding.

This paper presents a design method which utilizes Differential evolution optimization algorithm to obtain the optimal factors of axial and radial scaling that yield the scaled motor design with IE3 efficiency level and minimum volume of its lamination stack at the same time.

Scaling laws applied to induction motor design

Scaling laws describe the dependence of all relevant motor parameters and characteristics (resistances, inductances, current, power output, losses, efficiency etc.) on variation of the axial dimension (stack length) by the factor k_{A} and the radial dimensions (stator inner and outer diameter, air-gap length, width and height of stator and rotor slots and teeth, end winding length, rotor cage end ring height and width, yoke height, shaft radius) by the factor k_{R}. In order to maintain the constant air-gap flux density, rewinding must be also performed along with axial and radial scaling. The other quantities which are unaffected by scaling are rated frequency, number of poles, number of stator and rotor slots, winding type, coil pitch, winding factors, rotor bar skewing and the resulting skewing factor.

The scaling laws presented in this paper primarily involve the laws for calculation of equivalent circuit parameters. The reference used for determination of the new rated power is the assumption of equal temperature rise in the stator winding of the original and scaled motor. The power losses in a single slot of the stator winding of a scaled motor are given by

$$P'_{\mathrm{Cusl}} = R'_{\mathrm{sl}} I'^2 = \frac{1}{\sigma} \frac{z'_{\mathrm{sl}} l'_{\mathrm{Fe}}}{A'_{\mathrm{sl}} \frac{f_{\mathrm{fill}}}{z'_{\mathrm{sl}}}} \left(J' A'_{\mathrm{sl}} \frac{f_{\mathrm{fill}}}{z'_{\mathrm{sl}}} \right)^2 = \frac{f_{\mathrm{fill}}}{\sigma} l'_{\mathrm{Fe}} \cdot$$

(1)

$$A'_{\mathrm{sl}} J'^2 = \frac{f_{\mathrm{fill}}}{\sigma} k_{\mathrm{A}} l_{\mathrm{Fe}} k_{\mathrm{R}}^2 A_{\mathrm{sl}} J'^2 = P_{\mathrm{Cusl}} k_A k_R^2 \left(\frac{J'}{J} \right)^2$$

where R'_{sl} is the resistance of conductors inside a single slot, I' is the current per conductor, J is the current density of the original motor, J' is the unknown current density of the scaled motor, σ is the conductivity of copper, z'_{sl} is the number of conductors per slot, l'_{Fe} is the stack length, A'_{sl} is the cross section of the slot, and f_{fill} is the slot fill factor. The thermal resistance between the conductors and the teeth of the scaled motor is given by [6]

$$R'_{\mathrm{th}} == \frac{1}{\lambda} \frac{d_{\mathrm{i}}}{A'_{\mathrm{sw}}} = \frac{1}{\lambda} \frac{d_{\mathrm{i}}}{k_{\mathrm{R}} \left(2h_{\mathrm{s}} + b_{\mathrm{s}} \right) k_{\mathrm{A}} l_{\mathrm{Fe}}} = \frac{R_{\mathrm{th}}}{k_{\mathrm{R}} k_{\mathrm{A}}} \quad (2)$$

where d_{i} is the thickness of the slot insulation, λ is the thermal conductivity of the insulation, h_{s} is the slot height, b_{s} is the slot width, R_{th} is the thermal resistance of the original motor, and A'_{sw} is the area of the slot wall of the scaled motor. The thickness of the insulation d_{i} is constant independent of the machine size since it depends on the rated voltage. Assuming that the temperature rise $\Delta\vartheta$ in the slot of the original motor and the temperature rise $\Delta\vartheta'$ in the scaled motor are equal, one can write

$$\Delta\vartheta = P_{\mathrm{Cusl}} R_{\mathrm{th}}, \quad \Delta\vartheta' = P'_{\mathrm{Cu\,sl}} R'_{\mathrm{th}}$$

$$\Delta\vartheta' = P_{\mathrm{Cusl}} k_{\mathrm{A}} k_{\mathrm{R}}^2 \left(\frac{J'}{J} \right)^2 \frac{R_{\mathrm{th}}}{k_{\mathrm{R}} k_{\mathrm{A}}} = \Delta\vartheta k_{\mathrm{R}} \left(\frac{J'}{J} \right)^2 \quad (3)$$

$$\Delta\vartheta = \Delta\vartheta' \Rightarrow J' = J \frac{1}{\sqrt{k_R}}$$

which yields the relationship between current density in the original and scaled motor.

The scaling of the number of conductors per phase is derived from the back-EMF equation assuming constant air-gap flux density and hence constant back-EMF ($E'_1=E_1$) in both original and scaled motor. Assuming sinusoidal distribution of the air-gap flux density, the number of stator phase conductors connected in series in the scaled motor is given by

$$z'_1 = \frac{E'_1}{2,22k_{w1}f}\frac{p}{B_\delta k_A l_{Fe}}\frac{1}{k_R D} = z_1\frac{1}{k_R}\frac{1}{k_A} \tag{4}$$

where E'_1 is the fundamental rms back-EMF, p is the number of pole pairs, k_{w1} is the stator winding factor for fundamental component, B_δ is the peak fundamental flux density, and D is the stator inner diameter.

In general, a three-phase winding of the scaled motor can have a' parallel paths and the original motor has a parallel paths, so a ratio $k_{ap}=a'/a$ can be defined. The number of conductors per slot of the scaled motor is then

$$z'_{sl} = 3a'\frac{z'_1}{N_1} = \frac{3}{N_1}ak_{ap}\frac{z_1}{k_R k_A} = z_{sl}\frac{k_{ap}}{k_R k_A} \tag{5}$$

where N_1 is the number of stator slots. In most cases it is desirable to maintain equal flux densities in both original and scaled motor to ensure the same level of saturation. However, a moderate variation of the number of conductors in the scaled motor may be beneficial for the purpose of boosting its efficiency by altering the ratio of winding to iron losses. This can be achieved by multiplying z'_{sl} with a factor k_z ($0.95 \le k_z \le 1.05$) which is used as one of the optimization variables. Of course, z'_{sl} from (5) must be rounded to the nearest integer value, and it is preferable to be an even number in a double layer winding.

With the known z'_{sl} from (5) and using (3) the rated current of the scaled motor is given by

$$I'_{1n} = \frac{A'_{sl}f_{fill}J'a'}{z'_{sl}} = \frac{A_{sl}k_R^2 f_{fill}Jk_R^{-\frac{1}{2}}ak_{ap}}{z_{sl}\frac{k_{ap}k_z}{k_R k_A}} = I_{1n}\frac{k_R^{\frac{5}{2}}k_A}{k_z} \tag{6}$$

The rated current I'_{1n} is used in combination with parameters of the equivalent circuit of the scaled motor to find the value of rated slip of the scaled motor assuming the same voltage in the original and scaled motor. Once the rated slip is known, the rated power and torque of the scaled motor can be calculated. This approach will ensure equal temperature rise in the winding of the original and scaled motor within the accuracy of a simple thermal model given by (2) and (3).

Scaling of equivalent circuit parameters

The expression for the stator phase winding resistance of the scaled motor can be derived from the following set of equations considering (4) and (5):

$$R'_1 = \frac{1}{\sigma}\frac{\frac{z_1^2k_z^2}{k_R^2k_A^2}\left(k_A l_{Fe} + k_R l_{ew}\right)}{k_R^2 A_{sl}f_{fill}N_1} = R_{sl}\frac{k_z^2}{k_R^4 k_A} + R_{ew}\frac{k_z^2}{k_R^3k_A^2} \tag{7}$$

where l_{ew} is the length of the end coil, and R_{ew} is the resistance of the end winding.

The expression for the stator leakage reactance of the scaled motor can be written in the form

$$\begin{aligned} X'_{\sigma 1} &= 4\pi f\mu_0\left(\frac{z_1}{2}\frac{k_z}{k_A k_R}\right)^2\frac{k_A l_{Fe}}{p}\cdot \\ &\cdot\left[k'^{sat}_{Xst1}\left(\frac{\lambda_{sl}}{q}+\frac{\lambda_{tt1}}{q}\right)+k'^{sat}_{Xv1}\lambda_{v1}+\frac{k_R l_{ew}}{k_A l_{Fe}}\lambda_{ew}\right] \\ &= \frac{k_z^2}{k_A k_R^2}\left(k'^{sat}_{Xst1}X_{\sigma 1st0}+k'^{sat}_{Xv1}X_{\sigma 1v0}\right)+\frac{k_z^2}{k_A^2 k_R}X_{\sigma 1ew} \end{aligned} \tag{8}$$

where $X_{\sigma 1st0}$ is the unsaturated leakage reactance of the slot and tooth tip part, $X_{\sigma 1v0}$ is the unsaturated harmonic leakage reactance, $X_{\sigma 1ew}$ is the leakage reactance of the end winding part, q is the number of slots per pole and phase, λ_{s1}, λ_{tt1}, λ_{v1} and λ_{ew} are the slot, tooth tip, harmonic and end winding specific permeances respectively, k'^{sat}_{Xst1} is the saturation factor for stator slot and tooth tip leakage, and k'^{sat}_{Xv1} is the saturation factor for stator harmonic leakage. The specific permeances are constant because they are dependent on ratios of geometric parameters which are equally affected only by radial scaling.

The saturation of leakage paths depends on the slot current and affects the stator leakage reactance in most cases at values of slip higher than breakdown slip. According to Ampere's law applied to one flux line of leakage flux one can write

$$\left.\begin{aligned} \frac{B}{\mu_{Fe}}l_{mFe}+\frac{B}{\mu_0}l_{m\delta s} &= I_{sl} \\ \frac{B'}{\mu'_{Fe}}k_R l_{mFe}+\frac{B'}{\mu_0}k_R l_{m\delta s} &= I'_{sl} \end{aligned}\right\} B' = B \Rightarrow I'_{sl} = I_{sl}k_R \tag{9}$$

where B is the common flux density related to the flux line passing through iron and across the slot, I_{sl} is the slot current encompassed by the flux line, l_{mFe} and $l_{m\delta s}$ are the lengths of the flux paths through iron and across the slot respectively. If the same level of saturation is obtained in the original and scaled motor ($B=B'$), then slot current I'_{sl} must be scaled by k_R. If instead of slot current the linear current density around stator perimeter is used, then the following is valid

$$A'_1 = \frac{N_1 I'_{sl}}{D'\pi} = \frac{N_1 k_R I_{sl}}{k_R D\pi} = A_1 \tag{10}$$

The linear current density will be the same for the same level of saturation and hence the same values of saturation factors in the original and scaled motor. This result leads to a conclusion that saturation factors should be plotted as a function of A_1 as shown in Fig. 1. These plots are obtained by varying the slip in the SPEED PC-IMD software and calculating the corresponding A_1, k^{sat}_{Xst1} and k^{sat}_{Xv1} for the original motor. The PC-IMD uses Norman's method to calculate k^{sat}_{Xst1} [7]. Since levels of saturation may generally change in the scaled motor, it is required to calculate A'_1 from its equivalent circuit for an operating point of interest and use it as an argument to obtain k'^{sat}_{Xst1} and k'^{sat}_{Xv1} from the fitted curves.

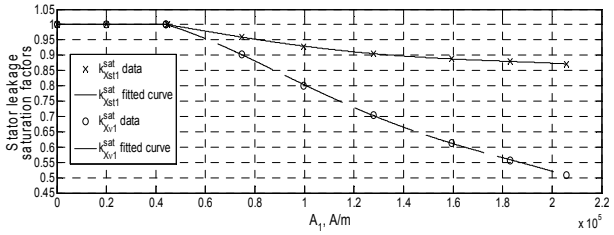

Fig. 1. Saturation factor for stator slot and tooth tip leakage and saturation factor for stator harmonic leakage

The magnetizing inductance of the scaled motor is given by

$$X'_{\mathrm{m}} = 2\pi f \mu_0 3 \frac{\alpha_i k_{\mathrm{R}} D k_{\mathrm{A}} l_{\mathrm{Fe}}}{2p^2 k_{\mathrm{c}} k_{\mathrm{R}} \delta} \left(\frac{k_{\mathrm{z}}}{k_{\mathrm{R}} k_{\mathrm{A}}} \frac{z_1}{2} k_{\mathrm{w1}} \right)^2 \frac{1}{k'_{X_{\mathrm{m}}}} = \frac{k_{\mathrm{z}}^2}{k_{\mathrm{R}}^2 k_{\mathrm{A}}} X_{\mathrm{m0}} \frac{1}{k'_{X_{\mathrm{m}}}} \tag{11}$$

where X_{m0} is the unsaturated magnetizing reactance of the original motor, α_{i} is the ratio of average and peak air gap flux density which takes into account flattening of the air gap flux density due to saturation, k_{c} is the Carter's factor, δ is the air-gap length, and k_{Xm} is the saturation factor. The factor k_{Xm} is calculated as a function of the air-gap flux density B_δ for the original motor (Fig. 2) by varying the slip in the SPEED PC-IMD software thus adjusting the stator current, voltage drop on the stator impedance and hence the value of the back EMF E_1 across the magnetizing reactance. The air-gap flux density of the scaled motor is then calculated using

$$B'_\delta = \frac{B_\delta}{k_{\mathrm{z}}} \frac{E'_1}{E_1} \tag{12}$$

and the value of k'_{Xm} is obtained from the fitted curve in Fig. 2 for the argument B'_δ. The back EMFs E_1 and E'_1 are calculated from the equivalent circuits of the original and scaled motor. In the scaled motor an iterative recursive scheme which converges very quickly is required since B'_δ depends on E'_1 which in turn depends of k'_{Xm}.

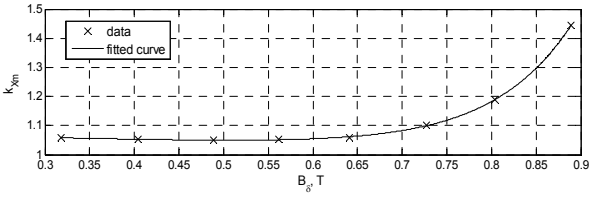

Fig. 2. Saturation factor for magnetizing reactance

The iron loss resistance depends on the back EMF and iron losses ($R_0 = 3E_1^2 / P_{\mathrm{Fe}}$). It can be assumed that flux density in the stator teeth and yoke of the scaled motor will alter with the same scaling factor as its air-gap flux density with respect to the original motor, i.e. $B'_\delta / B'_{\mathrm{Fe}} = B_\delta / B_{\mathrm{Fe}}$. Hence, for the scaled motor the following expression can be derived using (4) and assuming that hysteresis losses are proportional to the stator core flux density squared:

$$R'_0 = 3 \frac{\left(\frac{2,22 k_{\mathrm{w1}} f}{p} B'_\delta k_{\mathrm{R}} D k_{\mathrm{A}} l_{\mathrm{Fe}} \frac{z_1 k_{\mathrm{z}}}{k_{\mathrm{R}} k_{\mathrm{A}}} \right)^2}{k_{\mathrm{R}}^2 k_{\mathrm{A}} m_{\mathrm{Fe}} B'^2_{\mathrm{Fe}} \left(k_{\mathrm{h}} f_{\mathrm{s}} + k_{\mathrm{e}} f_{\mathrm{s}}^2 \right)} = \frac{k_{\mathrm{z}}^2}{k_{\mathrm{R}}^2 k_{\mathrm{A}}} R_0 \tag{13}$$

where m_{Fe} is the mass of the stator iron, k_{h} and k_{e} are the coefficients of hysteresis and eddy current losses.

The rotor resistance reduced to the stator consists of the slot part $R^{\mathrm{s}}_{\mathrm{2bar}}$ and end ring part $R^{\mathrm{s}}_{\mathrm{2er}}$. In the scaled motor the rotor resistance is given by

$$R'^{\mathrm{s}}_2 = \underbrace{\frac{3k_{\mathrm{w1}}^2 z_1^2}{N_2}}_{K_{\mathrm{r}}} \frac{k_{\mathrm{z}}^2}{k_{\mathrm{R}}^2 k_{\mathrm{A}}^2} \left(k'_{\mathrm{skinR}} \underbrace{\frac{1}{\sigma_{\mathrm{r}}} \frac{l_{\mathrm{bar}}}{A_{\mathrm{bar}}}}_{R_{\mathrm{2bar}}} \frac{k_{\mathrm{A}}}{k_{\mathrm{R}}^2} + \underbrace{\frac{2}{\sigma_{\mathrm{r}} \alpha^2} \frac{l_{\mathrm{er}}}{A_{\mathrm{er}}}}_{R_{\mathrm{2er}}} \cdot \frac{k_{\mathrm{R}}}{k_{\mathrm{R}}^2} \right) = \frac{k_{\mathrm{z}}^2}{k_{\mathrm{R}}^4 k_{\mathrm{A}}} k'_{\mathrm{skinR}} R^{\mathrm{s}}_{\mathrm{2bar}} + \frac{k_{\mathrm{z}}^2}{k_{\mathrm{R}}^3 k_{\mathrm{A}}^2} R^{\mathrm{s}}_{\mathrm{2er}} \tag{14}$$

where N_2 is the number of rotor slots, σ_{r} is the conductivity of rotor conductors, l_{bar}, A_{bar}, l_{er}, A_{er} are the lengths and cross sections of the bar and end ring respectively, R_{2bar} is the DC resistance of the rotor bar, K_{r} is the resistance reduction factor for the original motor, k'_{skinR} is the rotor bar resistance increase factor due to skin effect for the scaled motor, and $\alpha = 2\sin(p\pi/N_2)$ is the coefficient that allows algebraic addition of bar and end ring resistances. The skin effect correction factor can be calculated analytically for simple slot shapes like round or rectangular or a numerical multilayer approach [8] can be used for more complex slot shapes. In a rectangular slot this factor is a function of $\xi = h_{\mathrm{bar}} \sqrt{\pi f_{\mathrm{r}} \mu_0 \sigma}$ [8], where h_{bar} is the height of the rotor bar, f_{r} is the rotor current frequency and μ_0 is the permeability of vacuum. As an approximation this dependence is taken for all slot shapes to calculate k'_{skinR} according to the expression

$$\xi' = k_{\mathrm{R}} h_{\mathrm{bar}} \sqrt{\pi f_{\mathrm{r}} \mu_0 \sigma} = k_{\mathrm{R}} \xi \tag{15}$$

For the original motor k_{skinR} is calculated as a function of ξ (Fig. 3) using SPEED PC-IMD software by varying the slip s ($f_r = s \cdot f_{\mathrm{s}}$, f_{s} - stator frequency) and k'_{skinR} is calculated from the fitted curve for the new argument ξ' from (15). The skin effect correction factor for the rotor leakage reactance in the slot part k_{skinX} is calculated as a function of ξ (Fig. 3) in a similar manner as k_{skinR}.

The rotor leakage reactance reduced to the stator is influenced by skin effect and saturation. In the scaled motor it is calculated according to

$$X'^{\mathrm{s}}_{\sigma 2} = \underbrace{\frac{3k_{\mathrm{w1}}^2 z_1^2}{N_2}}_{K_{\mathrm{r}}} \frac{k_{\mathrm{z}}^2}{k_{\mathrm{R}}^2 k_{\mathrm{A}}^2} \cdot \left[k'^{\mathrm{sat}}_{\mathrm{Xst2}} k'_{\mathrm{skinX}} k_{\mathrm{A}} l_{\mathrm{Fe}} \lambda_{\mathrm{s2}} + k'^{\mathrm{sat}}_{\mathrm{Xst2}} \cdot k_{\mathrm{A}} l_{\mathrm{Fe}} \lambda_{\mathrm{tt2}} + \frac{2}{\alpha^2} k_{\mathrm{R}} l_{\mathrm{er}} \lambda_{\mathrm{er}} \right] = \frac{k_{\mathrm{z}}^2}{k_{\mathrm{R}}^2 k_{\mathrm{A}}} k'^{\mathrm{sat}}_{\mathrm{Xst2}} k'_{\mathrm{skinX}} \cdot X^{\mathrm{s}}_{\sigma 2\mathrm{sl0}} + \frac{k_{\mathrm{z}}^2}{k_{\mathrm{R}}^2 k_{\mathrm{A}}} k'^{\mathrm{sat}}_{\mathrm{Xst2}} X^{\mathrm{s}}_{\sigma 2\mathrm{tt0}} + \frac{k_{\mathrm{z}}^2}{k_{\mathrm{R}} k_{\mathrm{A}}^2} X^{\mathrm{s}}_{\sigma 2\mathrm{er}} \tag{16}$$

where $X^{\mathrm{s}}_{\sigma 2\mathrm{sl0}}$ and $X^{\mathrm{s}}_{\sigma 2\mathrm{tt0}}$ are the unsaturated rotor slot and tooth tip leakage reactances reduced to the stator, $X^{\mathrm{s}}_{\sigma 2\mathrm{er}}$ is the leakage reactance of the end ring reduced to the stator, λ_{s2}, λ_{tt2}, and λ_{er} are the slot, tooth tip and end ring specific permeances respectively, $k'^{\mathrm{sat}}_{\mathrm{Xst2}}$ is the saturation factor for rotor slot and tooth tip leakage. The specific permeances are constant like in the case of $X_{\sigma 1}$ because they are dependent on ratios of geometric parameters which are equally affected only by radial scaling. The variation of $k^{\mathrm{sat}}_{\mathrm{Xst2}}$ with rotor linear current density A_2 is shown in Fig. 4 and is obtained from SPEEED PC-IMD in the manner as $k^{\mathrm{sat}}_{\mathrm{Xst1}}$.

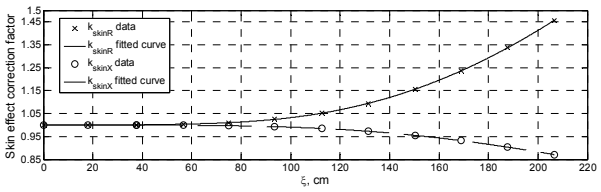

Fig. 3. Skin effect correction factor for rotor bar resistance and leakage reactance

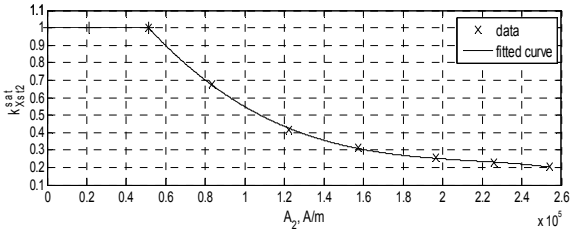

Fig. 4. Saturation factor for rotor slot and tooth tip leakage

Motor optimization using scaling laws

In the particular case presented in this paper the power rating of the original and scaled motor is kept constant at 4 kW and scaling laws combined with evolutionary optimization are used to calculate the equivalent circuit parameters and performance of geometrically scaled motor in a computationally quick and simple manner with the aim to reach the IE3 efficiency level (88,6 %) with minimum possible increase of the stack volume. The optimization variables are k_R, k_A and k_z. The minimum volume of iron stack is defined as a cost function. The additional constrains imposed on the scaled motor are the minimum allowed ratio of locked rotor torque to rated torque ($T_{LR}/T_n>4$), the maximum allowed ratio of locked rotor current to rated current ($I_{LR}/I_n\leq 9$), and the minimum allowed ratio of breakdown torque to rated torque ($T_{BR}/T_n\geq 4.5$). The original motor has a standard IEC lamination with 36 stator slots and 28 rotor slots.

The results of the optimization algorithm are summarized in Table 1. The performance of the scaled motor calculated using scaling laws has been compared to its performance calculated using SPEED PC-IMD software. The maximum difference is within 0.5 % for any of the parameters listed in the table thus confirming the reliability of the derived scaling laws.

Table 1. Comparison of performance of original and optimal motor calculated using SPEED PC-IMD and scaling laws

Optimal scaling factors: k_R=1.2879, k_A=0.6424, k_z=1.0024											
Parameter		Initial model	SPEED PC-IMD	Scaling laws	Error, %	Parameter		Initial model	SPEED PC-IMD	Scaling laws	Error, %
Stator outer diameter	D_{out}, mm	170	219	219	0.00	Stator leakage reactance	$X_{\sigma 1}$, Ω	9.319	9.322	9.321	0.01
Stack length	L_{Fe}, mm	160	102.8	102.8	0.00	Rotor resistance	R'_2, Ω	3.543	2.413	2.405	0.33
Stack volume	V_{stk}, mm^3	3632	3870	3870	0.00	Magnetizing inductance	X_m, Ω	121.1	114.5	114.7	0.17
Air-gap flux density	B_δ, T	0,88	0.879	0.8792	0.00	Core loss resistance	R_0, Ω	2417	2288	2279	0.39
No. conductors per slot	z_{sl}	39	189	189	0.00	Rated slip	s_n, %	3.87	2.60	2.59	0.39
Rated stator current	I_{1n}, A	5.10	5.18	5.17	0.19	Stator winding losses	P_{Cu1}, W	213.7	177.8	177.7	0.06
No-load current	I_0, A	2.97	3.14	3.14	0.00	Rotor winding losses	P_{Cu2}, W	163.1	108.1	107.7	0.37
Voltage across X_m	E_1, V	359.1	359.6	359.6	0.00	Iron losses	P_{Fe}, W	160.0	169.5	170.2	0.41
Input power	P_1, kW	4592	4514	4515	0.02	Magnetizing inductance	X_m, Ω	121.1	114.5	114.7	0.17
Shaft power	P_2, kW	4000	4000	4000	0.00	Efficiency	η	87.11	88.60	88.60	0.00
Rated speed	n_n, min^{-1}	1442.0	1461.1	1461.2	0.01	Power factor	$\cos\varphi$	0.750	0.727	0.727	0.00
Rated torque	T_n, Nm	26.49	26.14	26.14	0.00	Locked rotor torque	T_{LR}, Nm	125.0	104.8	104.6	0.19
Rotor leakage reactance	$X'_{\sigma 2}$, Ω	2.721	2.873	2.873	0.00	Locked rotor current	I_{LR}, A	42.2	45.5	45.5	0.00
Stator resistance	R_1, Ω	2.739	2.213	2.213	0.00	Breakdown torque	T_{BR}, Nm	131.6	130.1	130.0	0.08

Conclusion

The enhanced scaling laws for induction machines have been presented which take into account the variation of equivalent circuit parameters with radial and axial scaling of motor dimensions, rewinding, and saturation. Their practical implementation has been demonstrated on an example of design optimization of a 4 kW, 4-pole premium efficiency (IE3) squirrel-cage induction motor by utilizing radial scaling, axial scaling and rewinding of an existing high efficiency (IE2) motor. The equivalent circuit parameters and motor performance characteristics obtained by scaling show an excellent agreement with parameters and characteristics obtained from SPEED PC-IMD software.

Acknowledgment

This work was supported in part by the Croatian Science Foundation under the Project IP-11-2013-7801 Advanced Electric Drives for Traction Applications.

***Authors**: prof. dr. Damir Žarko, Stjepan Frljić, mag. ing. el. techn. inf., dr. sc. Stjepan Stipetić, University of Zagreb Faculty of Electrical Engineering and Computing, Unska 3, HR-10000 Zagreb, Croatia, E-mail: damir.zarko@fer.hr, stjepan.frljic@fer.hr, stjepan.stipetic@fer.hr*

REFERENCES

[1] R. Saidur, A review on electrical motors energy use and energy savings, *Renewable and Sustainable Energy Reviews*, 14 (2010), 877–898

[2] IEC 60034-30 Ed. 1 (2008): Rotating electrical machines - Part 30: Efficiency classes of single speed, three phase, cage-induction motors (IE code)

[3] L. Alberti, N. Bianchi, A. Boglietti, A. Cavagnino, Core Axial Lengthening as Effective Solution to Improve the Induction Motor Efficiency Classes, *IEEE Transactions on Industry Applications*, 50 (Jan.-Feb. 2014.), No. 1, 218-225

[4] J. C. H. Bone, Influence of Rotor Diameter and Length on the Rating Of Induction Motors, *IEE Journal On Electric Power Applications* 1 (Feb. 1978), No. 1, 2-6

[5] S. Stipetic, D. Zarko, M. Popescu, Ultra-fast axial and radial scaling of synchronous permanent magnet machines, *IET Electric Power Applications*, 2016, Available Online, DOI:10.1049/iet-epa.2016.0014

[6] J. Pyrhönen, T. Jokinen, V. Hrabovcová, *Design of Rotating Electrical Machines*, John Wiley & Sons 2014

[7] H. M. Norman, Induction motor locked saturation curves, *Trans. AIEE*, 53 (1934), 536-541

[8] I. Boldea, S.A. Nasar, *The Induction Machine Handbook*, CRC Press LLC 2002